

## Computation of the diffracted field by an elliptic rigid(/elastic) scatterer

D. Cassereau<sup>1</sup>, F. Mézière<sup>2</sup>, M. Muller<sup>2</sup>, E. Bossy<sup>2</sup> and A. Derode<sup>2</sup>

<sup>1</sup> *Laboratoire d'Imagerie Biomédicale, UPMC, CNRS, 75006 Paris, France, Email: didier.cassereau@upmc.fr*

<sup>2</sup> *Institut Langevin Ondes et Images, 1 rue Jussieu, 75005 Paris, France*

### Introduction & Context

This work is part of a more general study that aims at the numerical modelling of the ultrasonic propagation (with multiple scattering) in the trabecular bone. Trabecular bone is important as it is involved in the mechanical resistance of the bone itself, and also in the reconstruction mechanism after fracture. In this approach, we represent the internal structure of the trabecular bone by multiple independent scatterers. As the geometry of the bone structure is mainly based on long fibers of bone tissue, we simplify the model by replacing these structures by long elliptic elastic scatterers.

Typical dimensions of such elliptic scatterers are about  $700\mu\text{m} \times 100\mu\text{m}$ , with an ultrasonic inspection frequency of 1MHz. Based on these orders of magnitude, we clearly see that the individual scatterers are much smaller than the wavelengths.

The ISA theory is a simplified model that allows to describe multiple scattering, under some assumptions that are not discussed here. This model is based on the individual response of each scatterer, this is the reason why we feel concerned in this kind of computation.

### Computation with a FDTD code

The first simulations are based on the Finite-Difference Time-Domain (FDTD) code SimSonic [1] developed by E. Bossy. In all the following we only considered the 2D-case. SimSonic is used to calculate the propagation of a plane wave with and without the elliptic scatterer. It is then enough to evaluate the difference between the two resulting fields to obtain the contribution of the scattered pressure only. In this simulation, the elliptic scatterer can be either rigid or elastic, and is immersed in water.

The computation is done using staggered grids for stress and strain, with a spatial step size  $\Delta x$  that must be chosen small enough to describe precisely the external shape of the scatterer. From the CFL condition, we obtain the value of the temporal step  $\Delta t$  that ensures the stability of the numerical scheme. In addition to that, it is necessary to take into account PML conditions on the borders of the numerical domain, in order to avoid undesired reflections.

If we divide the spatial grid step  $\Delta x$  by 2, the amount of memory is multiplied by 4, and the total computation time by 8. This means that the computation cost can increase rapidly. For the purpose of this work, we have considered a spatial step  $\Delta x = 2\mu\text{m}$ . The total computation time is about 4 days on a 16-core Intel Xeon 64bits processor. The configuration is illustrated by Fig.(1).

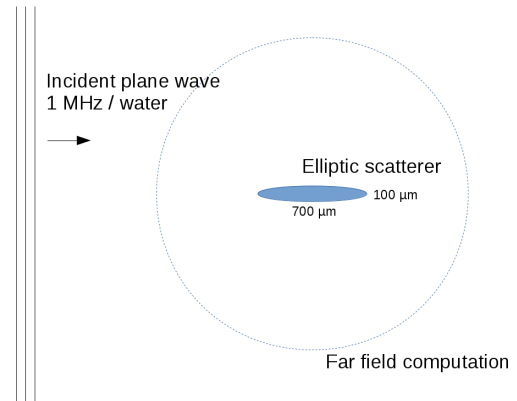


**Figure 1:** Computation of the scattered field with SimSonic

### Alternate approach: the modal decomposition

A classical formulation used for a circular scatterer is based on a decomposition of the incident and scattered field on a particular basis that is adapted to the shape of the scatterer. In this particular case, the cylindrical wave basis is particularly pertinent, therefore resulting in rewriting the incident plane wave as follows:

$$p_{inc}(r, \theta) = p_0 \sum_{n=-\infty}^{+\infty} i^n J_n(kr) e^{in\theta}$$

where  $(r, \theta)$  are the cylindrical coordinates of the observation point, and  $J_n$  the standard Bessel function of the first kind. Similarly the scattered field is then written as follows:

$$p_s(r, \theta) = p_0 \sum_{n=-\infty}^{+\infty} i^n A_n H_n^{(1)}(kr) e^{in\theta}$$

where  $H_n$  is the Hankel function of the first kind, and  $A_n$  the amplitude of the corresponding mode.

Writing the boundary conditions on the surface of the circular scatterer yields a linear system that allows the numerical computation of the coefficients  $A_n$ . Of course the infinite summation must be truncated, and the number of terms that are needed to ensure the convergence is classically known as being directly related to  $ka$ , product of the wave number (in the surrounding fluid) by the radius of the scatterer.

This formulation is adapted to the circular scatterer because the  $r$  and  $\theta$  variables are separable in the wave equation, and the border of the scatterer corresponds to a condition  $\{r = \text{constant}, \forall \theta\}$ .

Clearly these conditions are not satisfied for the elliptic

scatterer. A first solution consists in using elliptic coordinates: this allows to write a similar summation, based on Mathieu functions instead of the Bessel functions above. Unfortunately, this approach is not suitable for elastic scatterers. Another solution has been proposed by Chati *et al.* [4] that consists in a generalization of the circular formulation to the case of the elliptic scatterer. In this work, we have been interested in the evaluation of the limitations of this generalization.

The reader can refer to Chati *et al.* [4] for a detailed description of the proposed method. Basically it relies on a numerical integration of the boundary conditions over the surface of the elliptic scatterer. Of course the mathematical formulation is more complex than in the circular case, but the general principles remain unchanged. Once the boundary conditions are rewritten using the angular integration, we obtain a matrix to be inverted. This gives the values of the  $A_n$  coefficients, that can finally be used to calculate the scattered pressure.

**Practical implementation:** the proposed method has been implemented through a Matlab code to calculate the scattered pressure for various reference ellipses, as mentioned in Chati *et al.* [4]. The aspect ratio of the ellipse is 0.75 and  $ka \simeq 15 - 20$ , where  $a$  is the largest radius of the ellipse. Computation is fast, efficient, and provides results that have been confirmed experimentally. Applying the same code to our small ellipse  $100\mu\text{m}-700\mu\text{m}$  yields immediate huge difficulties:

- we do not observe any real convergence of the summation,
- the initial symmetry of the problem may be lost,
- Matlab prints diagnostic messages related to the `rcond()` number of the matrix,
- the matrix is very ill-conditioned due to the Bessel and Hankel functions.

With standard computer arithmetics (64 bits floating numbers), the relative precision is  $\varepsilon \simeq 1^{-16}$ : this means that the computer cannot differentiate 1 and  $1 + \varepsilon$ . The classical consequence of this is that the precision loss increase at each operation, particular when we have to manipulate numbers of different orders of magnitude. This is typically what happens here, where the Bessel function  $J_n$  rapidly tends to zero near the origin, while  $Y_n$  tends to infinity.

As the matrix is very ill-conditioned, the computation of its inverse is either impossible or yields erroneous results: the matrix is then numerically singular. This behavior also explains the loss of the original symmetry: the erroneous coefficients  $A_n$  used in the summation to calculate the scattered field produces a final result that is absolutely not significant.

## The use of extended precision

In all the following, we now only consider the particular case of a rigid scatterer, as the elastic situation may be significantly more complex.

One of the key points is the precision that results from standard arithmetics and is limited to 15-16 digits. The idea consists here in performing the same computation, but using an extended precision.

A first simple solution is to use 128bits floating numbers with a precision of 33 digits. Practically, in a problem like the one presented in this paper, we can rapidly observe that 33 digits are still not enough. Thus we have preferred a solution based on arbitrary precision.

Several numerical solutions can be tested:

- Python+mpmath: this solution works and can be easily implemented; the counterpart is that it is not very efficient in terms of the computation time,
- GMP+MPFR: GMP [2] is a free C library for arbitrary precision computation, and MPFR [3] is a free C++ class for GMP: all necessary functions exist (trigonometric functions, Bessel and Hankel functions), we just need to adapt the tanh-sinh integration rule to MPFR.

We have implemented and tested these three solutions, and finally retained the third one.

Whatever the solution we choose, the common counterpart of this kind of approach for numerical computation with arbitrary precision is the computation time, that may rapidly increase with the number of digits.

Figure (2) represents the modulus of the scattered pressure (far field, calculated at 10 mm from the center of the elliptic scatterer) in all observation directions for a given frequency  $f=1$  MHz. Figure (3) represents the same result using the modal decomposition with  $2 \times 50$  (blue curve), 100 (green curve), 200 (red curve) and 300 (black curve) terms. Comparing these two figures, we observe that the modal decomposition effectively converges to the expected solution, but requires a large number of terms (at least 200 in this particular case).

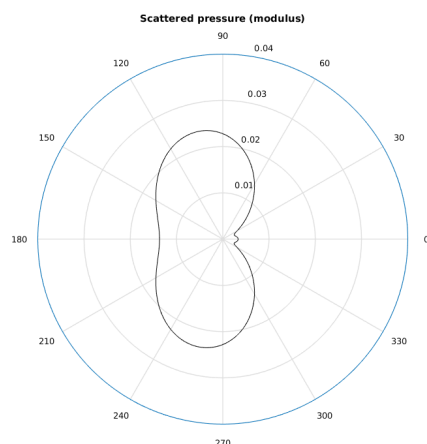


**Figure 2:** Computation of the scattered field with SimSonic

## The importance of precision

Based on the previous results, we have evaluated the influence of scattered field computation precision, observing that we aim at 300 terms in the summation. For that

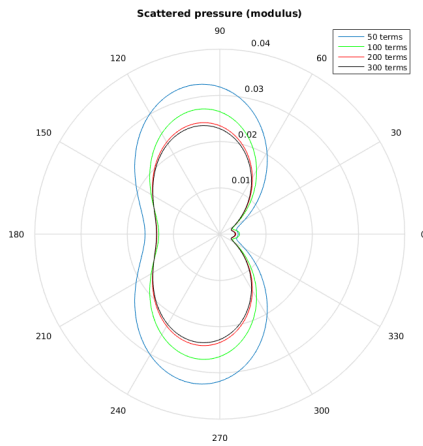


**Figure 3:** Computation with the modal decomposition using  $2 \times 50$ , 100, 200 and 300 terms

purpose, we calculate

$$\log \langle |p_{s,N+1}(\theta) - p_{s,N}(\theta)| \rangle_{\theta \in [0, 2\pi]}$$

This expression evaluates the influence of an additional term on the final result, averaged on the different values of the observation direction  $\theta$ , and consequently represents a quantitative evaluation of the convergence. Figure (4) represents the previous expression as a function of the number of terms  $N$  for 50 digits (blue curve), 100 digits (red curve) and 300 digits (green curve). For less than 130 terms, the three curves cannot be differentiated, this means that the three precisions give the same result. In this case, the use of 300 digits is of course not justified. After 130 terms, the blue curve starts showing a strange heratic behavior: the precision of 50 digits is no more enough, and we observe numerical instabilities. The red curve shows the same behavior near 270 terms, once again it means that after 270 terms, a precision of 100 digits is not enough to obtain a pertinent evaluation of the scattered pressure.

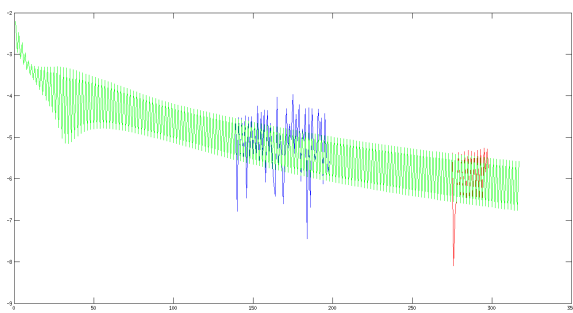


**Figure 4:** Influence of the precision

Table 1 gives the order of magnitude of the computation time, depending on the number of digits that have been used. A dedicated parallel scheme has been developed for this simulation, with  $\sim 150$  computation cores 24h a day. The total simulation has been run in one week of human time.

**Table 1:** Computation time

Precision	N	Matrix size	Computation time*
50 digits	130	$259 \times 259$	$\sim 7$ days
100 digits	270	$439 \times 439$	$\sim 45,5$ days
300 digits	320	$639 \times 639$	$\sim 766$ days

\*monoprocessor equivalent

## Evaluation of the number of terms

As we have seen above, it is important to have a good idea of the number of terms that will be needed in the modal decomposition to reach the numerical convergence, as this number of terms will then give a condition on the required precision that must be used. For that purpose, we have run multiple simulations with various elliptic objects with  $(ka, kb)$  varying in the domain  $[1, 10] \times [1, 10]$ . Here,  $a$  and  $b$  are the half-axes of the ellipses.

We first start with the diagonal of this domain, that corresponds to circular scatterers of increasing size. We introduce here a new quantitative evaluation of the convergence as

$$\log \left\langle \left| \frac{p_{s,N}(\theta) - p_{s,end}(\theta)}{p_{s,end}(\theta)} \right| \right\rangle_{\theta \in [0, 2\pi]}$$

where  $p_{s,end}$  is the solution obtained for a arbitrarily (and large enough) chosen maximum number of terms.

The blue curves on Fig. (5) illustrate the convergence for  $ka = 1$  (left) until  $ka = 10$  (right). The red and green curves correspond to small objects, with  $ka = 0.1$  and  $ka = 0.5$  respectively. All these curves show a first plateau (the number of terms is not large enough to ensure the convergence), followed by a break and a fast convergence. The position of the break clearly varies regularly and linearly with the size of the circular scatterer. This is a well-known result that the modal decomposition requires a number of terms that is around  $ka$ . This result applies only in the particular case of circular scatterers.

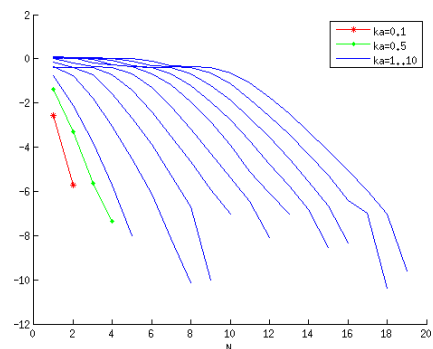


**Figure 5:** Convergence for circular scatterers,  $ka = kb$  increasing from 1 to 10

We now explore another portion of the domain: we start with  $ka = kb = 1$ , leave  $ka$  unchanged and increase  $kb$  to 10. The obtained result is shown on Fig. (6). For the purpose of comparison, the two red curves correspond to a small disk ( $ka = kb = 1$ ) and a large disk ( $ka =$

$kb = 10$ ) respectively. Then the blue curves correspond to  $kb = 2$  until  $kb = 10$ , from left to right.

Looking at this figure, we clearly see that the aspect ratio of the ellipse significantly influences the number of terms that are needed in the modal decomposition. In this particular situation, the number of terms of course depends on the size of the scatterer, but the aspect ratio is clearly dominant. We also see that for large aspect ratios, the number of terms becomes unreasonably high, based on the observations made in the previous section related to computation time.

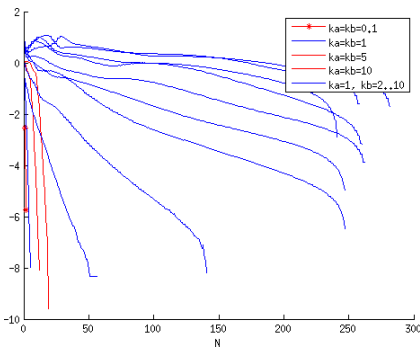


**Figure 6:** Convergence for elliptic scatterers,  $ka = 1$  and  $kb$  increasing from 1 to 10

The whole domain  $[1, 10] \times [1, 10]$  is represented by Fig. (7). For this figure, we have arbitrarily considered a convergence if the obtained solution differs from the final solution of less than 3%. This figure shows that the number of terms increase very fast, as soon as the aspect ratio of the ellipse becomes significantly different from 1. The same phenomenon is observed for large and small aspect ratios.

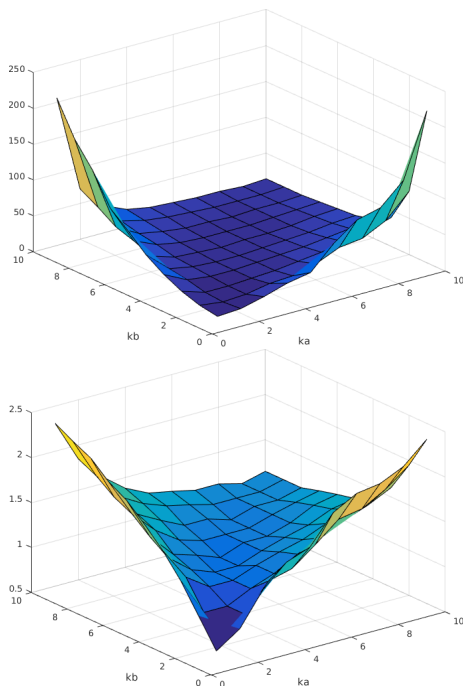


**Figure 7:** Convergence for elliptic scatterers (top: linear scale; bottom: log scale)

## Conclusions and perspectives

The first important conclusion is that the modal decomposition can be adapted for non-circular objects, but principally if the general shape of the object is not so far from a circle. Quantifying the "not so far" qualifier is not easy, as it depends on the computation time that can be considered as acceptable. Otherwise (and our example based on ellipses illustrates the problem), it may become very difficult to obtain the convergence, as it may require a large number of terms (the corresponding computation cost increase as  $N^2$ ), and consequently also a large precision (and this also contributes to a very large increase of the computation cost). Ellipses with a small or large aspect ratio cannot be considered as "smooth enough" to allow the use of this kind of approach.

We may understand this by observing the following points:

- for the circular scatterer, taking into account a new term in the summation just reduces to an additional term, in particular the previously computer coefficients do not change; this results from an orthogonality relationship between the different modes that appear in the decomposition,
- for the elliptic scatterer, this property is no more satisfied: modes are not orthogonal, and taking into account an additional term yields a change of all coefficients of the summation; this coupling between modes makes the convergence slow and difficult, and this effect is enforced by a large or small aspect ratio.

The particular case of the elliptic scatterer can also be addressed using a change of variable into elliptic coordinates. In this case, the modal summation is based on the Mathieu functions, in replacement of the Bessel and Hankel functions. The inconvenient of this alternate method is that i) it is mathematically complex and ii) it cannot be used with objects which are not elliptic. It also appears that the elliptic coordinates may be not adapted to the modelling of an elastic scatterer, due to the existence of two different propagation velocities.

Finally we are investigating a new numerical approach based on a conformal mapping method: this method starts to give very promising results, and could be applied for various object shapes, including flat and thin ellipses as described in this paper. This new approach will be investigated in the near future.

## References

- [1] SimSonic, URL: <http://www.simsonic.fr>
- [2] GMP, URL: <https://gmplib.org/>
- [3] MPFR, URL: <http://www.mpfr.org/>
- [4] Chati *et al.*, Modal theory applied to the acoustic scattering by elastic cylinders of arbitrary cross section, J. Acoust. Soc. Am **116**, 2004